GUIDED AND CONVECTED ACOUSTIC WAVE COUPLED WITH VIBRATING WALLS : WHAT KIND OF COUPLING ?

Vincent Martin

Centre National de la Recherche Scientifique, Institut Jean Le Rond d'Alembert, UMR7190, Université Pierre et Marie Curie, Place Jussieu, Paris, F
e-mail : vincent.martin@upmc.fr

Modelling the behavior of a guided and convected acoustic wave with one wall of the guide vibrating, it turns out that the coupling arises more likely through displacement than through velocity, a characteristic due to the convection. The subject is presented analytically for the physical understanding and extended in a numerical finite element model for releasing an analytical hypothesis. The influence of the flow Mach number is observed with both types of coupling to attempt to conclude on the more suitable coupling procedure.
Keywords: acoustic/structure coupling with convection

1. Introduction

The present theoretical work aims at providing arguments for choosing the coupling description of an acoustic wave convected by a flow within a duct with a vibrating wall of this duct.

Considering a duct of small rectangular cross-section with rigid walls the guided wave is plane only below the cut-off frequency unless the excitation imposes a plane wave, or if the modelling focuses on the plane wave only.

One of the walls is liable to vibrate due to the acoustic pressure applied on its inner face. This wall, in turn, radiates a sound pressure field within the duct. As far as plane waves are concerned, previous experiments confirmed predictions, in particular in a frequency range where the vibrating wall stops, or greatly attenuates, the acoustic wave by « pumping » it at the price of a high structural amplitude. The forbidden frequency range has long been well-known and then communicated [1,2].

Now the acoustic wave is convected by a stationary flow whose constant speed is along the axial direction of the duct only. Rigorously the description of the problem needs a flow profile such that its velocity at the walls would be zero were they rigid. For the sake of simplicity, a uniform flow is envisaged bending indeed the physical rules. At first sight the most natural way for the acoustic/structure coupling is to deal with the displacements (along the normal to the structure as no viscosity intervenes here) between both media at their interface. The numerical implementation of such a coupling proves to be more delicate than the coupling through the vibratory velocities, the latter usually being carried out (in numerical FE codes as well as in analytical procedures [3]). Without convection, the results are the same. It is no longer the case in presence of flow with the now transported acoustic pressure responsible for the vibration of the yielding wall. According to the type of coupling envisaged, the structural displacement or velocity is also transported, a counterintuitive fact. The previous simplication of uniform flow causes this drawback but it appears that the far more rigorous Ingard-Myers boundary condition arising from a deep analysis of the boundary layer does not yet prove to be a satisfactory description either [4].

Within the framework of the present hypotheses, what reasons justify a preference for one type of coupling rather to another, the intuitive displacement coupling alone being far from sufficient to be convincing ?

While fine academic experiments were carried out [4] for solving the inverse problem of identifying a liner impedance using the deduced convected wavenumbers (another inverse problem) from the measured acoustic pressure field, the present author is not aware of experimental results of the acoustic field when the liner impedance is given (direct problem). However, it is often heard that the maximum of attenuation significantly decreases when the flow velocity increases, while the frequency of this maximum seems to be shift toward higher values. Which coupling would confirm such tendencies (insofar as they have a certain degree of confidence) ?

2. Configuration and analytical description

In an attempt to answer the question posed, the flow speed V_0 is largely greater than the acoustic velocity (some tenths m/s against some cm/s).The simplest vibrating structure reacts locally like adjacent independant spring/mass systems ; it is called single degree of freedom liner. Honeycomb materials satisfy this modelling as a first approximation. The analytical model allows us to consider the contribution of the plane acoustic wave only. Figure 1 sketches the configuration of a partly lined duct with a stationary uniform flow.

The main focus is on the bandgap where acoustic evanescence or attenuation occur. It will be seen that :

- without any structural damping, i.e., with admittance only, the acoustic attenuation arises solely from the acoustic evanescence due to an exponential decreasing of the amplitude versus the distance with no propagation at all, therefore with a purely imaginary celerity;
- in presence of structural damping (resistance added to the admittance), the acoustic wave propagates with attenuation, with complex celerity;
- with flow and with/without structural damping, the bandgap is again no longer a forbidden frequency band since pure evanescence is replaced by attenuated propagation ; this point constitutes the new item of information that will be deepened here.

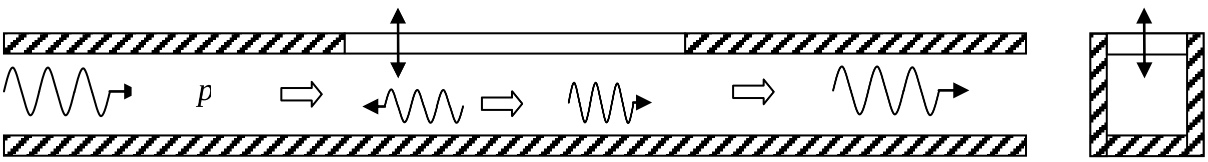

Figure 1 : A guide of infinite length has rigid walls except on a finite part where vibrations occur. A flow carries the acoustic wave. An acoustic incident pressure excites the global system.

For analytical modelling the acoustic wave should be plane or, said differently, this modelling reveals what phenomenon the plane wave can lead to [1,2]. As usual, a combination of dynamic, mass conservation and state laws result in the wave equations, presently, Eqs. (1) and (2) respectively through coupling via displacement and velocity.

$$p_{,yy} - \frac{\rho_0}{S}\int_P \ddot{w}_{st}(y,l,t)\ dl - \frac{1}{c^2}\ddot{p} = 0 \qquad (1)$$

$$p_{,yy} - \frac{\rho_0}{S}\int_P \dot{v}_{st}(y,l,t)\ dl - \frac{1}{c^2}\ddot{p} = 0 \qquad (2)$$

with y axial direction ; $p(y,t)$ acoustic pressure ; $u_{,y}$ or $\partial_y u$ and $u_{,yy}$ or $\partial_{yy} u$ resp. first and second partial space derivatives of u ; $\dot{u}$ and $\ddot{u}$ resp. first and second time material derivatives of u ; w_{st} and v_{st} resp. structural displacement and vibratory velocity (along the outward normal to the structure); c air sound speed; ρ_0 air density; S cross-section area; P wall's vibrating perimeter.

Harmonic (in the frequency-space domain) spectral coupling operators, without excitation and for the infinite guide with an infinitely long vibrating wall, take the form of Eqs. (3) and (4) resp. whether coupling occurs with displacement or velocity. In fact the basis is made up of the first two lines, what follows is mere developement where $\overline{u}$ describes the average value of $u(l)$ along the vibrating perimeter P i.e., $\overline{u} = \frac{1}{P}\int_P u(l)\ dl$). Morevover we have: V_0 flow speed ; M Mac number ; k acoustic wavenumber in the air; ω circular frequency; Z impedance of the structure (in the form of an acoustic impedance p/v) made up of its reactance X and resistance R s.t., $Z = R + iX$, the reduced value (in the acoustic sense) of which is $Z^{red} = \frac{Z}{\rho_0 c}$. Equations (5) and (6) give the formulations in acoustic pressure only, after removing the structural velocity.

Reactance expands in $X = m_{st}\omega - \frac{k_{st}}{\omega} = m_{st}\left(\omega - \frac{\omega_{st}^2}{\omega}\right) = \rho_{st} h\left(\omega - \frac{\omega_{st}^2}{\omega}\right)$ with ρ_{st} , h, m_{st} , k_{st} , ω_{st} , resp. structure density, thickness, mass, stiffness and eigen(circular)frequency. This impedance can also be measured via the Kundt duct method without requiring more details. So doing, a honeycomb material $34mm$ thick has an eigenfrequency of $1900Hz$ and a reduced impedance up to $3200Hz$. On a duct of small cross-section ($4\text{x}4cm^2$, first cut-off frequency $4287Hz$) this leads to a tremendous unmeasurable attenuation, suitable for theoretical investigations only.

$$\left\{\begin{array}{l}
\left\{\begin{array}{l} p_{,yy} - \frac{\rho_0 P}{S}\ddot{\overline{w}}_{st}(y) - \frac{1}{c^2}\ddot{p} = 0 \\ i\omega Z\overline{w}_{st} = p \end{array}\right. \\
\left\{\begin{array}{l} p_{,yy} - \frac{\rho_0 P}{S}\left(-\omega^2 + 2i\omega V_0\partial_y + V_0^2\partial_{yy}\right)\overline{w}_{st}(y) - \frac{1}{c^2}\left(-\omega^2 + 2i\omega V_0\partial_y + V_0^2\partial_{yy}\right)p = 0 \\ i\omega Z\overline{w}_{st} = p \end{array}\right. \\
\left\{\begin{array}{l} \left(1 - M^2\right)p_{,yy} - 2ikMp_{,y} + \omega^2\frac{\rho_0 P}{S}\overline{w}_{st}(y) - 2ik\frac{\rho_0 P}{S}cV_0\partial_y\overline{w}_{st}(y) - \frac{\rho_0 P}{S}V_0^2\partial_{yy}\overline{w}_{st}(y) + k^2 p = 0 \\ i\omega Z\overline{w}_{st} = p \end{array}\right.
\end{array}\right. \quad (3)$$

$$\left\{\begin{array}{l}
\left\{\begin{array}{l} p_{,yy} - \frac{\rho_0}{S}\int_P \dot{v}_{st}(y,l,t)\ dl - \frac{1}{c^2}\ddot{p} = 0 \\ Zv_{st} = p \end{array}\right. \\
\left\{\begin{array}{l} p_{,yy} - \frac{\rho_0 P}{S}d_t\overline{v}_{st}(y,t) - \frac{1}{c^2}\ddot{p} = 0 \\ Z\overline{v}_{st} = p \end{array}\right. \\
\left\{\begin{array}{l} p_{,yy} - \frac{\rho_0 P}{S}\frac{1}{Z}\left(i\omega + V_0\partial_y\right)p - \frac{1}{c^2}\left(-\omega^2 + 2i\omega V_0\partial_y + V_0^2\partial_{yy}\right)p = 0 \\ Z\overline{v}_{st} = p \end{array}\right.
\end{array}\right. \quad (4)$$

$$\left(1-M^2+i\frac{\rho_0 P V_0^2}{SZ\omega}\right)p_{,yy}+2i\left(-kM+i\frac{\rho_0 P V_0}{SZ}\right)p_{,y}+\left(k^2-i\omega\frac{\rho_0 P}{SZ}\right)p=0 \tag{5}$$

$$\left(1-M^2\right)p_{,yy}+i\left(-2kM+i\frac{\rho_0 P V_0}{SZ}\right)p_{,y}+\left(k^2-i\frac{\rho_0 P\omega}{SZ}\right)p=0 \tag{6}$$

These ordinary differential spectral equations (5) and (6) with constant coefficients (relative to space) provide the dispersion curves through solving the related second order algebraic characteristic equations, tackled by hand or by a software, here Mathematica.

3. Analytical dispersion curves and comments

For plane acoustic waves only, the dispersion graphs on Figs. 2a,b,c and 3a,b,c show the sound speeds within the duct according to frequency (from the characteristic equation roots) for a structure without/with damping without/with flow for coupling through displacement or velocity. Second order algebraic equations result in two complex speeds: real part in red, imaginary part in black; positive and negative resp. for waves going to and fro.

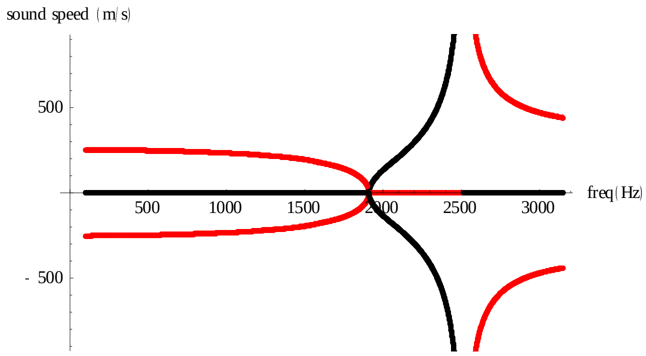

Figure 2a : Structure without damping and Mach 0.

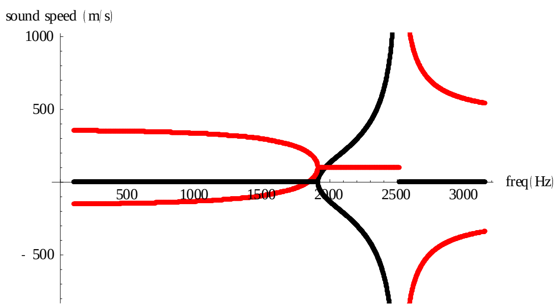

Figure 2b : Structure without damping at Mach 0.3.Coupling through displacement.

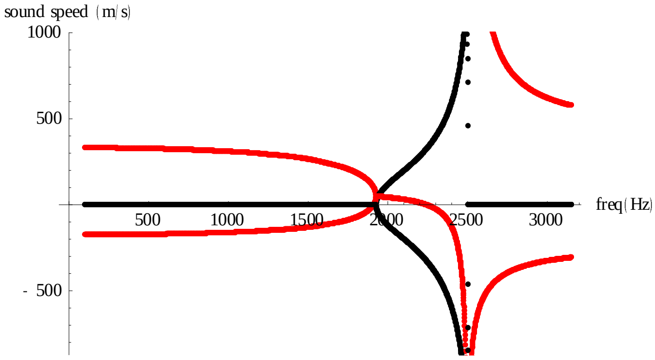

Figure 2c : Structure without damping at Mach 0.3. Coupling through velocity.

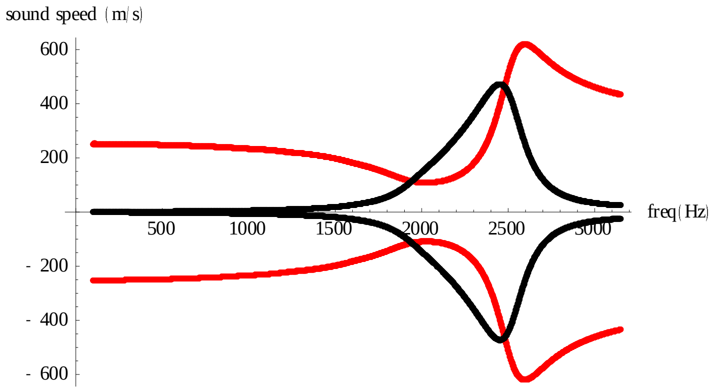

Figure 3a : Structure with damping and Mach 0.

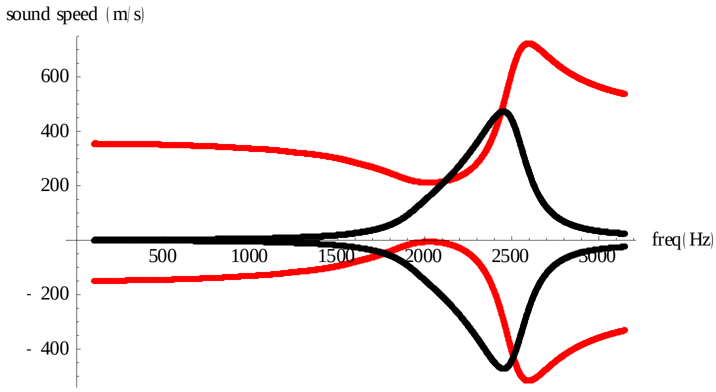

Figure 3b : Structure with damping at Mach 0.3.Coupling through displacement.

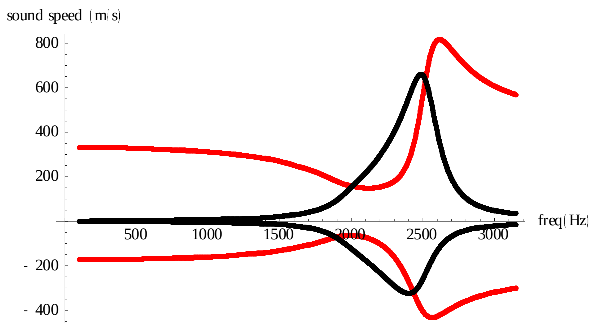

Figure 3c : Structure with damping at Mach 0.3. Coupling through velocity.

Figure 2a has long been well-known. Both waves to and fro travel with the same celerity (of course) and the forbidden frequencies range circa between $1900-2500Hz$ with a purely evanescent wave, located between the eigenfrequency of the structure isolated and the same frequency modified by the added acoustic stiffness related to the acoustic load brought by the air within the duct. Below the range, we find a subsonic zone, and above a supersonic zone.

Figure 3a reveals the deformation of Fig. 2a due to structural damping. The bandgap is replaced by a slightly larger domain with an attenuated propagation; maximum attenuation is below $2500Hz$.

On Figs.2b,c and 3b,c with flow the sound speed is no longer the same for the wave propagating upstream (smaller real speed) and dowstream (greater real speed). Figures 2b,c present similar subsonic and supersonic zones while they differ greatly in the « old » bandgap. With the coupling carried out via the displacement, the propagation speed is that of the flow: the previous evanescent wave of Fig. 2a is transported by the flow, thus ruining the bandgap. On Fig. 2c the coupling through velocity results in a change of sign of the sound speed indicating that the wave changes direction at a certain frequency, a surprising fact. Why ?

Figures 3a and 3b/c read in terms of wavenumbers versus frequency show, roughly speaking, some characteristics of Fig.s 3a,b in [4] (the comparison could benefit from using the same data).

Focusing on the imaginary speeds for an undamped structure, analysis by hand of solutions of Eqs. (5)-(6) bring two items of information. Coupling via displacement results in the speeds arising from inequality $k^2 - \frac{\rho_0 \omega P}{SX} \leq 0 \; \forall M$; the frequency range does not depend on the flow speed. It is demonstrated that the attenuation is the same in both directions. Coupling via velocity leads to the range for $k^2 - \frac{\rho_0 \omega P}{SX} + \frac{1}{4}\left(\frac{\rho_0 P V_0}{SX}\right)^2 \leq 0$ depending now on the flow speed (Fig. 2c does not put into evidence graphically this analytical property) but attenuation again is the same in both directions.

With structural damping (Fig.3b) the enlargment of the frequency band with attenuation - a property essential to point out the interest of attenuation through coupling - compensates the loss of the pure bandgap. Graphical inspection shows the same attenuation in both directions for displacement coupling while this is not the case with velocity coupling (Fig. 3c). The latter seems strange. What causes it ?

With damping, analysis by hand of the solutions, difficult, did not give properties.

Actually, at this stage of the analytical exploration, the displacement coupling shows :

- a pure transport of the evanescent wave due to the existence of a flow ;
- a attenuation that does not depend on the direction of propagation (when a flow exists) ;

while the velocity displacement leads to strange phenomena :

- a change in direction of propagation within the frequency range with attenuation ;
- a greater attenuation dowstream than upstream.

4. Analytical transmission loss

Section 3 focused on the *potential* solutions *before* a sollicitation intervenes. The phenomena at play stemmed from the roots of these solutions. What would be the acoustic field in presence of an excitation due to an incident acoustic plane wave? The answer provided analytically is partial since it takes into account the plane acoustic wave component only. Moreover the eventual properties so put into evidence reveal global behavior far less fundamentally than those previously presented.

The operator worked on arises from Eq. (5) or (6) now applied to the finite domain with the vibrating wall and provided with acoustic boundary conditions :

$$\begin{cases} p_{,y} - ik_u p = -i(k_d + k_u) p_{inc} \text{ for } y = y_1 \text{ at the entry of the finite domain} \\ p_{,y} + ik_d p = 0 \text{ for } y = y_2 \text{ at the output of the finite domain} \end{cases} \tag{7}$$

The first condition expresses the arrival of an incident pressure wave transported by the flow with wavenumber k_d and reflected upstream with wavenumber k_u ; the second describes a unique convected presssure wave leaving the finite domain in dowstream direction.

Such an operator is easily solved: two waves propagate to and fro within the finite domain with appropriate wavenumbers deduced from the dispersion curves on Figs. 2 and 3; their amplitude results from the two boundary conditions. Presently the acoustic field property takes the form of the transmission loss TL , here identical to the insertion loss, defined by $TL_{dB} = 20 \log_{10} \frac{|p(y_2)|}{|p_{inc}|}$. Let us point out that attenuation now originates from the acoustic/structure coupling, from the structural damping, and from the impedance break at interface of the finite domains on both its left and right side, therefore potentially reducing the importance of the only acoustic/structure coupling part.

The graphs of the TL versus frequency with the Mach number as a parameter, with coupling through displacement and velocity are given on Figs. 4. The structure used for the illustration is that of Section 3: honeycomb material $34mm$ thick and $50cm$ long, that led to dispersion curves on Figs. 3b/c. Such a material coupled with a guide of so small a cross-section is tremendously efficient; such an unmeasurable TL lends itself to theoretical work rather than practical for the time being.

The very first obvious global property observed is on the attenuation decreasing as the velocity flow increases, considerably for displacement coupling, less so for velocity coupling. Morevover the frequency of highest attenation shifts rightward as flow speed increases. Were the experimental assertions true and sustained by fine academical works, the displacement coupling would abound in this experimental direction. A final observation: the curves in Fig. 3b,c would imply an notable attenuation around $2500Hz$ at the highest imaginary wave speed, while the maximum TL goes frome $2000Hz$ to $2200Hz$ approximately.

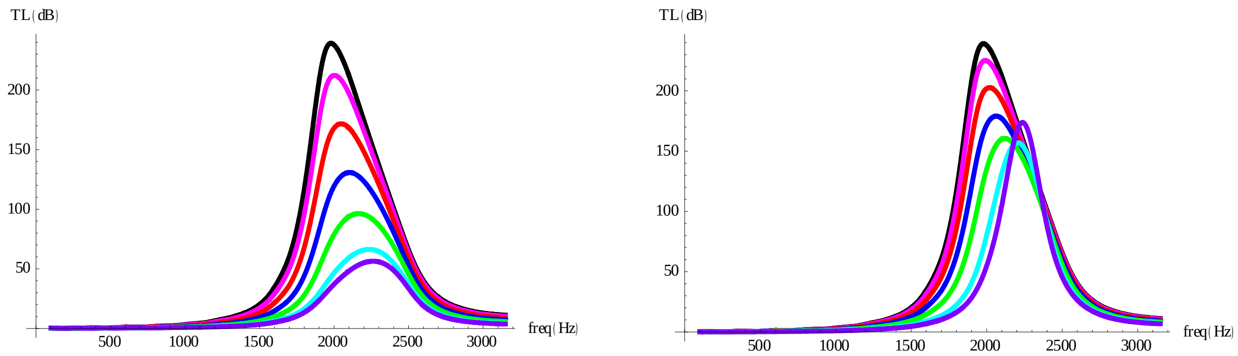

Figure 4: Analytical TL (dB) versus frequency (Hz).
(black :M=0, magenta :M=0.05, red :M=0.15, blue :M=0.3, green :M=0.5, turquoise :M=0.8, violet :M=0.95). Left :coupling through displacement. Right : coupling through velocity.

To conclude on this Section 5, it seems that, as long as only the plane acoustic wave is concerned :

- the TL decreases notably when the flow speed increases, this far more notably for the displacement coupling ;
- both couplings induce a rightward shift of the frequency of maximum attenuation ;
- perhaps, displacement coupling could be more convincing if experimental results indeed establish the same facts.

5. Numerical transmission loss

To disregard the restrictive hypothesis due to the plane acoustic wave within the finite domain with vibrating wall, 3D finite element numerical modelling is appropriate. However, to take into account the boundary conditions such as those in Eqs. (7), the acoustic wave must be plane outside the finite domain, an hypothesis satisfied below $4387Hz$ with the present duct. There is no room here to develop the finite element formulation but, despite its technical aspects, it owns interests from the mathematical approximations at play. Its analysis will be carried out in another framework.

Removing the plane acoustic wave hypothesis in front of the vibrating structure, Figs. 5 give the TL versus frequency for various flow speeds. As a first observation, maximum of attenuation occurs at a frequency lower than with the analytical TL. No reason has been found. It is true also that maximum attenuation decreases as the flow speed increases and is again accompanied by a frequency shift toward the right. Surprising results occur at very high mach number for coupling through displacement. Moreover, coupling through velocity proves to be very similar to that through displacement in contradiction with analytical conclusions. Will the future analysis of the numerical code give insight into these latter surprising results ?

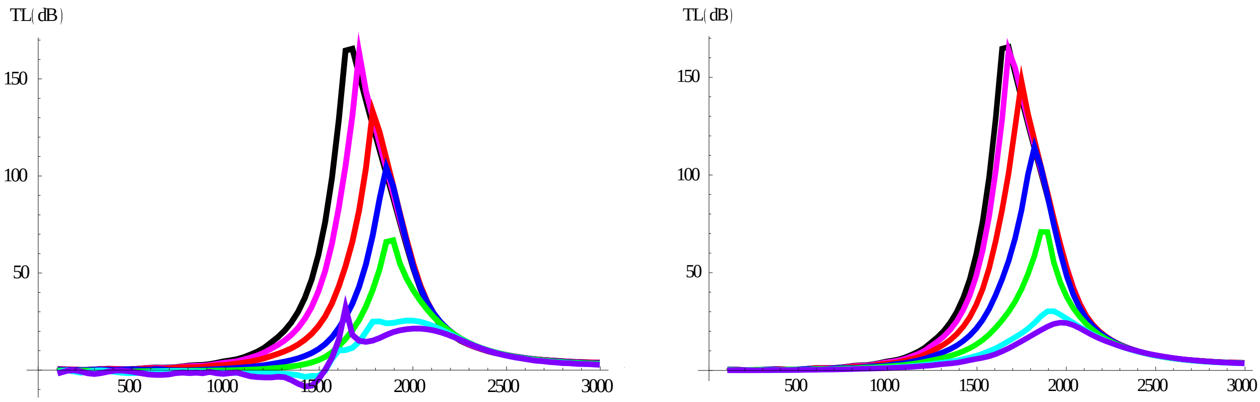

Figure 5: Numerical TL (dB) versus frequency (Hz).
(black :*M*=0, magenta :M=0.05, red :*M*=0.15, blue :*M*=0.3, green :M=0.5, turquoise :M=0.8, violet :M=0.95). Left :coupling through displacement. Right : coupling through velocity.

6. Conclusion

In the present configuration coupling through displacement could be more suitable than through velocity when resting on physical properties deduced from the dispersion curves (analytical).

The existence of global property in the *TL* form is not that clear in absence of fine experimental results. While plane acoustic wave hypothesis in the domain with vibrating wall results in a clear difference between the two couplings, ignoring this hypothesis seems to remove this difference. A deeper numerical analysis is necessary.

So, the question posed is still challenging even if the present work contributes somewhat to the answer.

REFERENCES

1. Morse P.M., Ingard K.U., *Theoretical Acoustics*, Section 9.1, Para « Ducts with yielding walls », MacGraw-Hill, Inc., (1968).

2. Martin V., *Eléments d'acoustique générale*, Section 18.1, Presses Polytechniques et Universitaires Romandes, (2007).

3. Liu Y., Choy Y.S., Huang L., Cheng L., Reactive control of subsonic axial fan noise duct, *Journal of the Acoustical Society of America*, **136**(4), 1619-1630, (2014).

4. Renou Y. , Aurégan Y., Failure of the Ingard-Myers boundary condition for a lined duct : An experimental investigation, *Journal of the Acoustical Society of America*, **130**(1), 52-60, (2011).

Acknowledgment

The author is indebted to his close academic colleagues M. Ben Tahar (Pr.), F. Gauthier (Pr.) and G. Pavic (Pr.) for exchanging ideas on the subject; and also thanks M. Versaevel (Ing., Safran-Nacelles Industry) for providing the reduced impedance of the honeycomb material.